

# Providing a Revenue-forecasting Scheme to Relocate Groups of Ride-Sourcing Drivers

Caio Vitor Beojone\* and Nikolas Geroliminis

Urban Transport Systems Laboratory (LUTS), École Polytechnique Fédérale de Lausanne (EPFL), Lausanne, CH-1015, Switzerland

## SHORT SUMMARY

Proper positioning of ride-sourcing drivers may improve vacant travel times, waiting times, and matching opportunities. Herein, we evaluate the potential repositioning response of drivers when provided a guidance based on estimates of their earnings in a system offering ride-hailing (solo) and ridesplitting (shared) rides. We develop a strategy that enumerates the best regional repositioning destination based on the expected number of requests. A mixed continuous-discrete time Markov Chain (MDCTMC) is developed to predict drivers activities and the revenues associated with them. Our main findings indicate that the proposed approach is likely to retain drivers confidence by improving their earnings compared to other drivers. We also show that it manages to decrease the number of unserved requests compared to several state-of-art benchmarks and decreased the deadheading.

**Keywords:** Macroscopic Fundamental Diagram; Markov chain; Shared mobility; Urban mobility.

## 1 INTRODUCTION

In a daily basis, geographical variations on the demand can create an imbalance between the ride-sourcing service demand and supply of drivers to serve it, requiring actions to maintain a satisfactory service quality. However, the fleets of this service are formed by drivers that are free to make a series of decisions.

Therefore, the operator requires persuasion to relocate the available pool of drivers. Sadeghi & Smith (2019), and Powell et al. (2011) incentivized drivers to decide on the location for the next assignment. However, these strategies suffer from a reactive nature, mainly accounting for past events. For instance, if an area faces recurrent losses of requests, customers will likely change their travel option.

Other strategies emerge from the optimization of passenger-driver matching algorithms. These strategies include Alonso-Mora et al. (2017) who sent empty vehicles to the location of recently unsatisfied customers. Other examples can be found in Wang & Yang (2019) and references therein. More recent studies, try to take actions before losing these passengers. Zhu et al. (2022) uses coverage control to proactively position idle drivers. Although proactive, these approaches assume full compliance, ignoring the individual objectives of human drivers.

From all the above, multiple challenges arise when positioning ride-sourcing currently available drivers. The first challenge is to take the burden of identifying the most profitable options from drivers with limited information, which only have access to limited information while accounting for drivers' future activities. A challenge remains in giving positions that minimizes unnecessary overlapping in demand coverage among drivers. Finally, the strategy must ensure that compliant drivers have an improved outcome to ensure compliance.

Herein, we evaluate the potential repositioning response of drivers when provided an estimate of their earnings. The operator uses a mixed discrete-continuous time Markov chain (MDCTMC) to estimate individual earnings for a given decision in the short-term. A microscopic process identifies the positions and paths with the highest chances of matching. In a simulated study, we compared the performance of guided drivers and unguided ones. We show that guided drivers have increased revenues and are likely to follow the provided guidance in the long term. Finally, the proposed strategy is compared to state-of-art strategies, achieving superior results in terms of lost requests and deadheading.

## 2 IDENTIFYING THE BEST REGIONAL REPOSITIONING DECISIONS

Assume that the objective of the repositioning strategy is to maximize the driver's revenues by maximizing the number of requests served during a short prediction horizon  $\tau$ . Therefore, the driver moves from the current position  $i$  to the potential position  $j$  for a significant portion of the prediction. Then, we can summarize the expected number of requests a driver can cover  $P_{ij}(t)$  in this period as shown in Equations [1] and [2]. Finally, Equation [3] indicates the chosen path for the driver.

$$P_{ij}(t) = \sum_{o \in \mathcal{R}} \sum_{d \in \mathcal{R}} P_{ij}^{od}(t) \quad (1)$$

$$P_{ij}^{od}(t) = \int_t^{t+\tau} p_{ij}^{od}(s) ds \quad (2)$$

$$\arg \max_j P_i = P_{ij}(t) \quad (3)$$

Where  $P_{ij}^{od}(t)$  and  $p_{ij}^{od}(t)$  represent the number of requests and the demand rate with a regional OD-pair  $od$  covered in the path between driver's current location  $i$  and potential repositioning destination  $j$ , respectively.

For the computation of the instantaneous covered demand rates  $p_{ij}^{od}(t)$  we consider: (i) geographical distribution of demand, (ii) the associated path, and (iii) other drivers' demand coverage. Figure 1 depicts these elements.

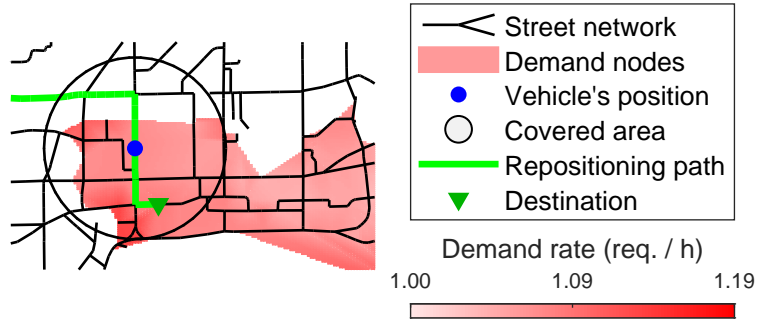


Figure 1: Illustration of the computation of  $p_{ij}^{od}(t)$ .

## 3 PROVIDING DRIVERS WITH REPOSITIONING GUIDANCE BASED ON REVENUE FORECASTING

While drivers decide about repositioning by themselves, they have incomplete information about the system conditions. Therefore, it is more likely that the service provider, who concentrates information about all drivers and demand can use the mobile application to supply drivers with repositioning information. The idea is to present the driver with the expected best decisions whenever he becomes available for relocation.

### *Predicting drivers' activities*

Since ride-sourcing drivers offer rides for a profit, one should expect their decisions aiming to maximize it. Therefore, to convince drivers about the best decisions they should be presented with the consequence of their choices on their earnings.

To predict the earnings, it must identify the driver's activities and actions in the near-future. Inspired by Beojone & Geroliminis (2022), consider a list of activities  $\mathbb{A}$ , such that  $A \in \mathbb{A}$  indicates a driver's current activity. A set  $\mathcal{R}$  with  $R$  heterogeneous regions, i.e.,  $\mathcal{R} = \{1, 2, \dots, R\}$  illustrate the urban network area, while the pair  $od \in \mathcal{R}^2$  depicts a driver's current and destination regions. Therefore,  $A_{od} \in \mathcal{K}$  describes a driver current state in the set of all possible states. Setting the list of activities  $\mathbb{A} = \{I, RH, S1, S2\}$  assumes that a driver can execute the following four activities completing the state-space with a size  $|\mathcal{K}| = |\mathbb{A}| \cdot |\mathcal{R}|^2$ .

- Vacant ( $I$ ): a vacant driver available for passengers.
- Ride-hailing ( $RH$ ): a busy driver assigned to a ride-hailing passenger.
- Single ridesplitting ( $S1$ ): a driver assigned to a single ridesplitting passenger.
- Shared ridesplitting ( $S2$ ): a driver assigned to two ridesplitting passengers.

Assuming that the time spent in each activity is random, a Markov chain can depict a driver's movements. If the operator has detailed information on the urban area, then it can accurately tell the time a driver needs to reach different areas in their repositioning activities.

Based on the previous, we can break a driver's activity predictions into three phases. In the first phase ( $a$ ), a continuous time Markov chain (CTMC) represents the movements of a driver before reaching the subsequent region in the repositioning path. In the second phase ( $b$ ), a discrete time Markov chain (DTMC) represents the driver reaching the boundary of the current region. Lastly, in the third phase ( $c$ ), after a driver reached the destination region, he is once again free to get any assignments in the network. Therefore, obtaining a construct referred as a mixed discrete-continuous time Markov chain (MDCTMC) model (Ingolfsson, 2005).

### ***Repositioning movements: phase (a)***

The provided shortest path is summarized in the sequence of regions  $\mathbf{r} = (r_1, r_2, \dots, r_n)$  the driver will cover on the movement between regions  $o$  and  $d$  ( $r_1 = o$  and  $r_n = d$ ). Therefore, the transitions in phase ( $a$ ) include those from the starting region  $o$  until the current region  $l$ . Equation [4] further details the dynamics for state probabilities  $\pi_{ij}^K(t)$ .

$$\dot{\pi}_{ij}^I(t) = -\pi_{ij}^I(t) \sum_{s \in \mathcal{S}} \lambda_{ij}^s(t) \quad (4a)$$

$$\dot{\pi}_{ij}^{RH}(t) = -\pi_{ij}^{RH}(t) \mu_{ij}^{RH}(t) + \pi_{ij}^I(t) \lambda_{ij}^H(t) \quad (4b)$$

$$\dot{\pi}_{ij}^{S1}(t) = -\pi_{ij}^{S1}(t) \left( \mu_{ij}^{S1}(t) + \sum_{h \in \mathbf{r}} \beta_{ij}^h \lambda_{ih}^S(t) \right) + \pi_{ij}^I(t) \lambda_{ij}^{S1}(t) + \pi_{ij}^{S2}(t) \vartheta_{ij}(t) \mu_{ij}^{S2} \quad (4c)$$

$$\dot{\pi}_{ij}^{S2}(t) = -\pi_{ij}^{S2}(t) \mu_{ij}^{S2}(t) + \sum_{h \in \mathcal{R}} \hat{\lambda}_{ihj}^{S2}(t) \quad (4d)$$

Where the base transitions can be described through the arrival process  $\lambda_{od}^s(t)$  for a service  $s \in \mathcal{S} = \{H, S\}$  (ride-hailing and ridesplitting), and the service process  $\mu_{od}^K(t)$ , in which driver completes a ride or transfers to a neighboring region. Note that any  $\mu_{ij}^K(t)$  and  $\lambda_{ij}^s(t)$  is only defined for  $j = d$  and  $i \in r_1, \dots, r_{n-1}$ , otherwise they have a value of 0.  $\beta_{od}^h$  represents the ratio of  $od$  trips that will pass through region  $h$ .  $\vartheta_{ij}$  indicates the probability of the driver in  $S2_{ij}$  having a passenger to deliver in  $i$  before proceeding to  $j$  with the other one.

### ***Repositioning boundary: phase (b)***

The DTMC of phase ( $b$ ) is depicted in Equation [5], which is supported by Equations [6] and [7] detailing the transition matrix. Note that the only change from the end of phase ( $a$ ) occurs from state  $I_{id}$  to  $I_{ld}$ , whereas the remaining states keep the same probabilities. Since the travel time to reach region  $l$  is assumed deterministic, the transition occurs with certainty.

$$\pi(t^+) = B(i, d, l) \pi(t^-) \quad (5)$$

$$B(i, d, l) = [b_{ij}^K(i, d, l)] \in \mathbb{B}^{|\mathcal{K}| \times |\mathcal{K}|} \quad (6)$$

$$b_{ij}^K(i, d, l) = \begin{cases} 1, & \text{for } K_{ij} = I_{ld}, RH_{id}, S1_{id}, S2_{id}, S2_{ih} \\ 0, & \text{otherwise} \end{cases}, \quad (7)$$

Where  $t^+$  and  $t^-$  refer to the instant right after and right before time  $t$ .  $B(i, d, l)$  is the transition matrix representing the DTMC.  $\mathcal{K}$  is the state space of the model, and  $|\mathcal{K}|$  is its cardinality.

### After repositioning: phase (c)

Once the driver reaches the area intended in the repositioning decision, it becomes free to answer any requests and a CTMC (different from phase(a)) depicts its activities. Figure 2 illustrates the state space of a single region and the possible transitions. In the figure, regions ‘k’ and ‘h’ can be a set of regions immediately before or after region ‘o,’ respectively.

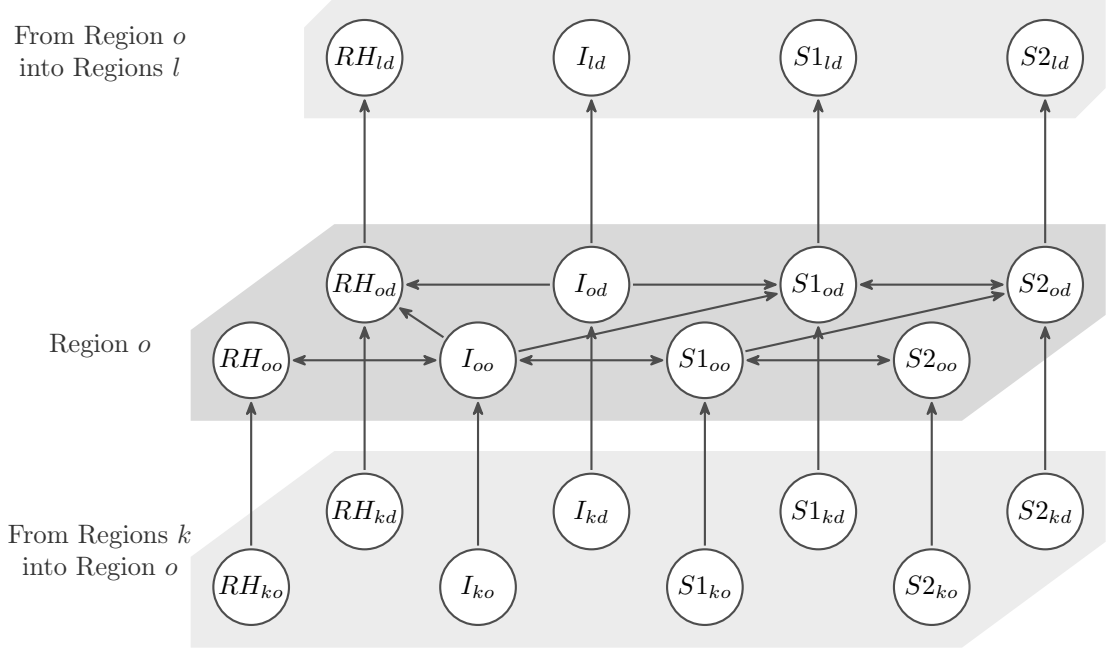


Figure 2: General state transition structure focusing on a region  $o$  and the inflows and outflows related to this region.

Therefore, we can describe the CTMC with the respective Equation 8, where we estimate the state probability  $\pi_{od}^K(t)$ . Table 1 provides the entries for each state in the CTMC.

$$\dot{\pi}_{od}^K(t) = - \text{Exits} + \text{Entrances} \quad (8)$$

State	Exits	Entrances
$I_{oo}$	$\pi_{od}^I(t) \sum_{s \in \mathcal{S}} \sum_{h \in \mathcal{R}} \lambda_{oh}^s(t)$	$\pi_{oo}^{RH} \mu_{oo}^{RH}(t) + \pi_{oo}^{S1}(t) \mu_{oo}^{S1}(t)$
$I_{od}$	$\pi_{od}^I(t) \sum_{s \in \mathcal{S}} \lambda_{od}^s(t)$	$\sum_{h \in \mathcal{R}} \hat{\mu}_{hd}^I(t)$
$RH_{od}$	$\pi_{od}^{RH}(t) \mu_{od}^{RH}(t)$	$\sum_{h \in \mathcal{R}} \pi_{oh}^I(t) \lambda_{od}^H(t) + \sum_{h \in \mathcal{R}_o} \hat{\mu}_{hod}^{RH}(t)$
$S1_{od}$	$\pi_{od}^{S1}(t) \mu_{od}^{S1}(t) + \hat{\lambda}_{ohd}^{S2}(t) + \hat{\lambda}_{odh}^{S2}(t)$	$\sum_{h \in \mathcal{R}} \pi_{oh}^I(t) \lambda_{od}^S(t) + \sum_{h \in \mathcal{R}_o} \hat{\mu}_{hod}^{S1}(t) + \hat{\mu}_{od}^{S2}(t)$
$S2_{od}$	$\pi_{od}^{S2}(t) \mu_{od}^{S2}(t)$	$\sum_{h \in \mathcal{R}} \hat{\lambda}_{ohd}^{S2}(t) + \sum_{h \in \mathcal{R}_o} \hat{\mu}_{hod}^{S2}(t)$

Table 1: Summary of state transitions in the Markov Chain model.

We have to detail the entries of the coefficients for ‘Exits’ and ‘Entrances,’ in Equation [8]. To shorten the description in Table 1, we aggregated some particular transitions explained in Equations [9]–[13]. In particular, Equation [9] illustrates that a driver can use different paths on his way to the destination. Equations [10] and [11] illustrate that shared ridesplitting drivers might complete a ride (Equation [10]) before transferring (Equation [11]). Finally, Equations [12] and [13] illustrate

that new shared ridesplitting rides can have different delivery order, such as a *last-in-first-out* (LIFO) order (Equation [12]) or a *first-in-first-out* (FIFO) order (Equation [13]).

$$\hat{\mu}_{hod}^K(t) = \pi_{hd}^K(t) \cdot \theta_{hod} \cdot \mu_{hd}^K(t) \quad K \neq S2 \quad (9)$$

$$\hat{\mu}_{od}^{S2}(t) = \pi_{od}^{S2}(t) \cdot \vartheta_{ood}(t) \cdot \mu_{od}^{S2}(t) \quad (10)$$

$$\hat{\mu}_{hod}^{S2}(t) = \pi_{hd}^{S2}(t) \cdot (1 - \vartheta_{ood}(t)) \cdot \theta_{hod} \cdot \mu_{hd}^{S2}(t) \quad (11)$$

$$\hat{\lambda}_{ohd}^{S2}(t) = \pi_{od}^{S1}(t) \cdot \beta_{od}^h \cdot \lambda_{oh}^S(t) \quad (12)$$

$$\hat{\lambda}_{odh}^{S2}(t) = \pi_{od}^{S1}(t) \cdot \beta_{oh}^d \cdot \lambda_{oh}^S(t) \quad h \neq d \quad (13)$$

Where,  $\theta_{hod} \in [0, 1]$  distributes transfer flows over its neighboring regions such that the equality  $\sum_{h \in \mathcal{R}_o} \theta_{ohd} = 1$  holds;  $\vartheta_{ood}$  becomes the fraction of shared trips passing through  $o$  that will deliver a passenger before continuing to  $d$ ; and  $\beta_{od}^h$  ( $\beta_{oh}^d$ ) represents the ratio of  $od$  ( $oh$ ) trips that will pass through region  $h$  ( $d$ ).

Note that there are two forms of transition processes, generally represented by  $\lambda_{od}^s(t)$  and  $\mu_{od}^K(t)$  for the passenger assignment rate and trip completion/transfer rates, respectively. These are translations of the macroscopic transitions in Beojone & Geroliminis (2022) to the individual level.

### ***Estimating drivers' expected revenues***

Drivers' earnings come from the fares passengers pay when booking rides, which are composed by a couple of elements. Firstly, there is a fixed booking fee  $f_{od}^{s,B}$  relative to the reservation of a ride. Secondly, there is a travel fee relative to the trip distance  $f_{od}^{s,T}$ . The platform keeps a commission  $\kappa$  for this fare and returns to the drivers the remaining part.

From the MDCTMC, one can approximate the revenue generation by means of a continuous rate. Therefore, a driver receives a part of the fees proportionally to the number of received assignments during the evaluation and to the kilometers traveled in busy states. Equation [14] summarizes the expected revenue after commission  $\kappa$ . However, it requires us to break the gross revenue into its minor components throughout Equations [15] – [21].

$$E[R^{\text{net}}] = (1 - \kappa)E[R] \quad (14)$$

$$E[R] = E[R^B + R^T] = E[R^B] + E[R^T] \quad (15)$$

$$E[R^B] = E \left[ \sum_s R^{s,B} \right] = \sum_s E [R^{s,B}] \quad (16)$$

$$E[R^{s,B}] = E \left[ \sum_{od \in \mathcal{R}} R_{od}^{s,B} \right] = \sum_{od \in \mathcal{R}^2} E [R_{od}^{s,B}] \quad (17)$$

$$E[R_{od}^{s,B}] = E \left[ f_{od}^{s,B} n_{od}^{s,B} \right] = f_{od}^{s,B} E [n_{od}^{s,B}] \quad (18)$$

$$E[R^T] = E \left[ \sum_s R^{s,T} \right] = \sum_s E [R^{s,T}] \quad (19)$$

$$E[R^{s,T}] = E \left[ \sum_{od \in \mathcal{R}^2} R_{od}^{s,T} \right] = \sum_{od \in \mathcal{R}^2} E [R_{od}^{s,T}] \quad (20)$$

$$E[R_{od}^{s,T}] = E \left[ f_{od}^{s,T} d_{od}^{s,T} \right] = f_{od}^{s,T} E [d_{od}^{s,T}] \quad (21)$$

Where  $n_{od}^{s,B}$  is the number of booked rides for service  $s$  from region  $o$  to region  $d$ ; and  $d_{od}^{s,T}$  is the passenger-distance traveled for a service  $s$  from region  $o$  to region  $d$ .

Finally, Equations [22] and [23] estimate the remaining expected number of booked rides and passenger-distance travelled based on the instantaneous probabilities from the MDCTMC. In summary, these estimates are functions of a starting time  $t_0$  and an evaluation period  $\tau$  for a particular choice  $\gamma$ .

$$E[n_{od}^{s,B}(t_0, \tau|\gamma)] = \int_{t_0}^{t_0+\tau} \lambda_{od}^s(t) \sum_{K \in \mathcal{K}_B^s} \pi_{od}^K(t) dt \quad \mathcal{K}_B^s = \begin{cases} \{I, RP\}, & \text{if } s = H, \\ \{I, RP, S1\}, & \text{if } s = S \end{cases} \quad (22)$$

$$E[d_{od}^{s,T}(t_0, \tau|\gamma)] = \int_{t_0}^{t_0+\tau} v_o(t) \sum_{K \in \mathcal{K}_T^s} n_p^K \pi_{od}^K(t) dt \quad \mathcal{K}_T^s = \begin{cases} \{RH\}, & \text{if } s = H, \\ \{S1, S2\}, & \text{if } s = S \end{cases} \quad (23)$$

Where  $n_p^K$  is the number of assigned passengers to a driver in activity  $K$ . For states  $RH$  and  $S1$ ,  $n_p^K = 1$ , while for  $S2$  have  $n_p^{S2} = 2$ .

## 4 COMPUTATIONAL RESULTS

In this prototype application, we represented the central business district of Shenzhen, including parts of the Luohu and Futian Districts. The considered network consists of 1'858 intersections connected by 2'013 road segments. The experiment used a simulator based on Bejone & Geroliminis (2021, 2022), using Floy-Warshall algorithm to compute shortest paths and a Speed-MFD to estimate average traveling speeds. A network-weighted  $k$ -mean algorithm separated the area into three distinct regions and the Speed-MFD data (Figure 3).

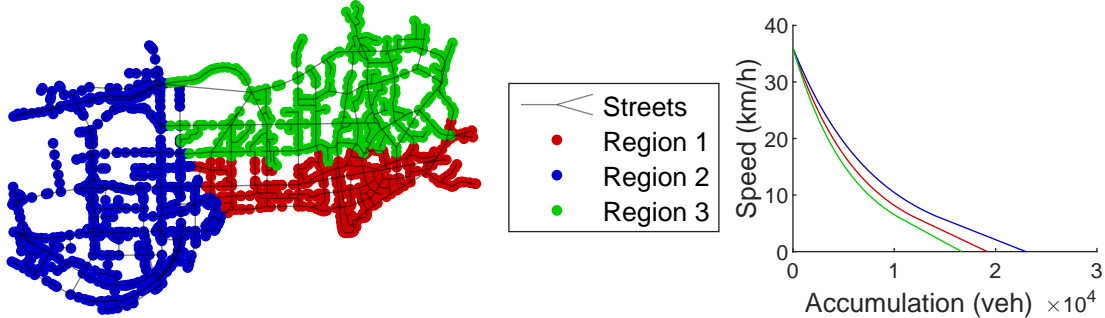


Figure 3: Settings of the experiments. (Left) urban area map and regions with respective centroids of the  $k$ -mean problems. (Right) Regional speed-MFD.

We assume a non-homogeneous Poisson arrival process for all travelers in the area to highlight the effects of imbalanced demand. Note that around 85% of arriving travelers use private vehicles, while the remaining use one of the ride-sourcing service options.

### *Sensitivity analysis*

The first analysis of the repositioning strategy focused on the sensitivity to the fraction of drivers receiving the repositioning guidance. One can correlate such scenarios with the operator selecting a groups of drivers for a ‘loyalty program’, and as part of the benefits, these drivers receive improved guidance in their search for assignments. In the direction of this parallel, we refer to drivers which receive guidance as ‘guided’ ones, whereas the others are referred as ‘unguided’.

We assume a logit decision process, where the utility of each option is depicted exclusively by the revenue it generates to a ‘guided’ driver. Finally, we define that ‘unguided’ drivers look for the region with the highest demand per driver rate (similar to a ‘high demand’ flag in current ride-sourcing operations).

Additionally, we evaluated the results for fleet sizes of 2000, 2500 and 3000 active drivers in ride-sourcing services. We ran cases with 0%, 25%, 50%, 75% and 100% of drivers covered in the ‘loyalty program’. As final parameters, we considered booking fares of US\$2.20 and US\$2.00, and traveling fares of US\$1.00 and US\$0.80 for ride-hailing and ridesplitting, respectively.

Since the proposed repositioning framework must persuade ‘guided’ drivers, their outcomes should be higher than those of ‘unguided’ drivers. Figure 4 shows the average revenues of both groups of drivers at different guidance rates (fraction of the fleet that receives repositioning guidance information). Firstly, average revenues increased compared to a scenario where drivers never relocate in all cases with guidance (the exception occurs at 0% guidance rate). We must point out

that guided drivers consistently had higher revenues than non-compliant ones. It highlights that the proposed framework captured the possibility of areas with lower demand being more profitable. However, it is interesting to observe that as the operator expands the number of ‘guided’ drivers (more than 75% of the fleet), the combined average revenue slightly decreases.

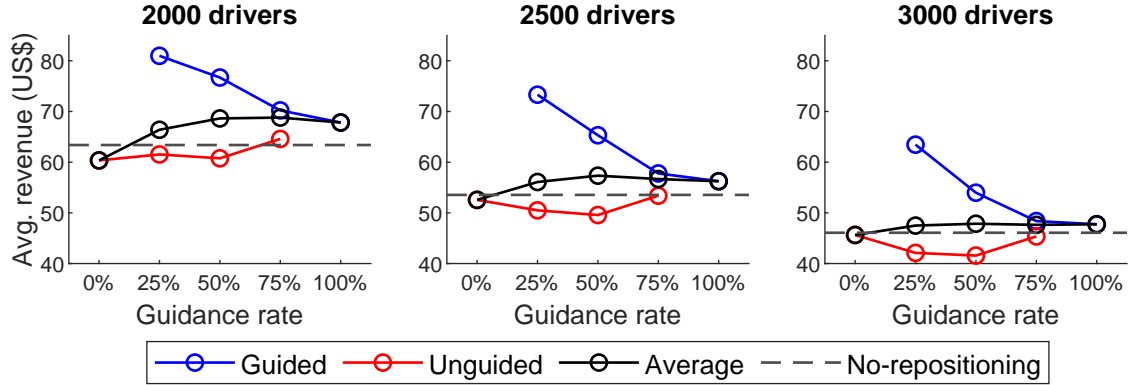


Figure 4: Average revenues of ‘guided’ and ‘unguided’ drivers following by a combination of these in scenarios with different penetration rates of the loyalty program, compared to the base ‘No-repositioning’ case.

It is interesting to take a closer look at individual revenues and understand their distribution. Figure 5 shows the histograms of the revenues for ‘unguided’ and ‘guided’ drivers in the base ‘No-repositioning’ scenario and one with 25% guidance ratio for a service fleet of 2000 drivers. With a left skewed distribution, no repositioning scenario had lower average revenue average. In the scenario with 25% of ‘guided drivers, the distribution of revenues was unimodal with the average close to the mode, creating a clear distinction between the groups. The average revenue of compliant drivers was higher than the revenue of 97% of non-compliant ones.

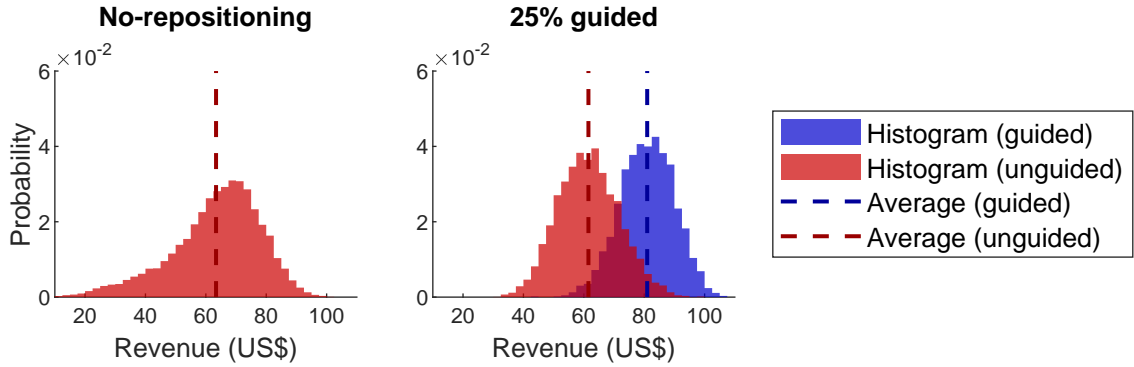


Figure 5: Histograms of revenues in two separated instances with 2000 drivers.

### Benchmark comparisons

As argued earlier, other repositioning strategies exist to improve service quality but they can fall short on their reactive nature and/or full compliance assumptions. Here, we position the proposed strategy in comparison with other benchmark strategies. In addition to the ‘No-repositioning’ base case and the ‘Proposed’ strategy, we evaluate the strategies named below:

1. ‘Past-revenue’: Provides a portion of ‘guided’ drivers with an average revenue estimation accounting exclusively for past events in each area;
2. ‘Past-loss’: Dispatches the closest idle driver to the area of a recently lost request (Alonso-Mora et al., 2017);
3. ‘Coverage’: Performs optimal coverage control, distributing idle drivers according to the demand distribution in the area (Zhu et al., 2022);

It is important to highlight that the ‘Past-revenue’ strategy has a reactive nature but allows drivers to decide, whereas ‘Past-loss’ strategy is reactive and assumes full compliance with the instructions. Foremost, the objective of repositioning vehicles is to improve the service quality, especially by making the service available in previously uncovered areas. Figure 6 compares the number of unattended service requests (abandonments) for all evaluated strategies. Firstly, when no drivers receive guidance and base their decisions on ‘high-demand areas’ information (0% guidance) it, actually, worsened the service increasing abandonments compared to the base case. Reactive strategies (‘Past revenues’ and ‘Past losses’) performed poorly, with little to no improvement compared to the base case. The most interesting point goes to comparison between the ‘Proposed’ and the ‘Coverage’ approaches. Although optimized, the ‘Coverage’ approach was outperformed by the ‘Proposed’ approach with a 50% guidance ratio, decreasing abandonments by 61% for a fleet of 2000 vehicles. Nevertheless, there are small increase in abandonments if guidance ratio is higher than 50%, which highlights the limitations the individualized decision-making towards service quality.

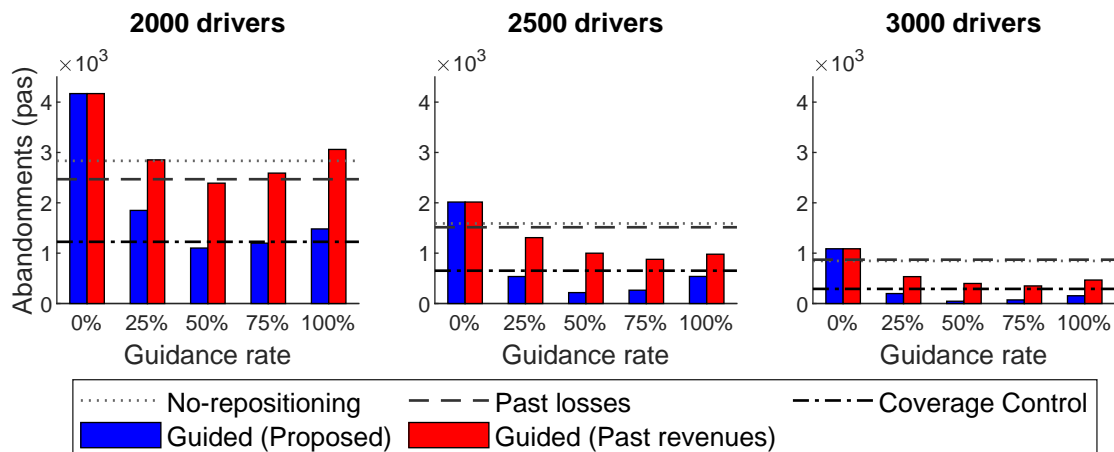


Figure 6: Summary of passenger abandonment results for all compared strategies.

In a different direction, most attention to ride-sourcing effect over congestion goes to their dead-heading. In Figure 7, we summarize the deadhead accumulated for each strategy for the same tested cases with 2000 vehicles and 50% guidance ratio. The only strategy to increase it, both in the unassigned and pick-up activities, is the ‘Past-revenues’ strategy. In the ‘Proposed’ approach, the unassigned deadhead is minimized but the ‘Coverage’ approach minimized the ‘Pick-up’ deadhead. It highlights two distinct points about of these strategies. First, while the ‘Proposed’ approach maximizes the chances of a drivers being assigned, the driver only needs to be as close as passengers’ waiting time tolerance accepts. Second, ‘Coverage’ approach had minimal ‘Pick-up’ deadhead because it “mimics” the expected demand distribution.

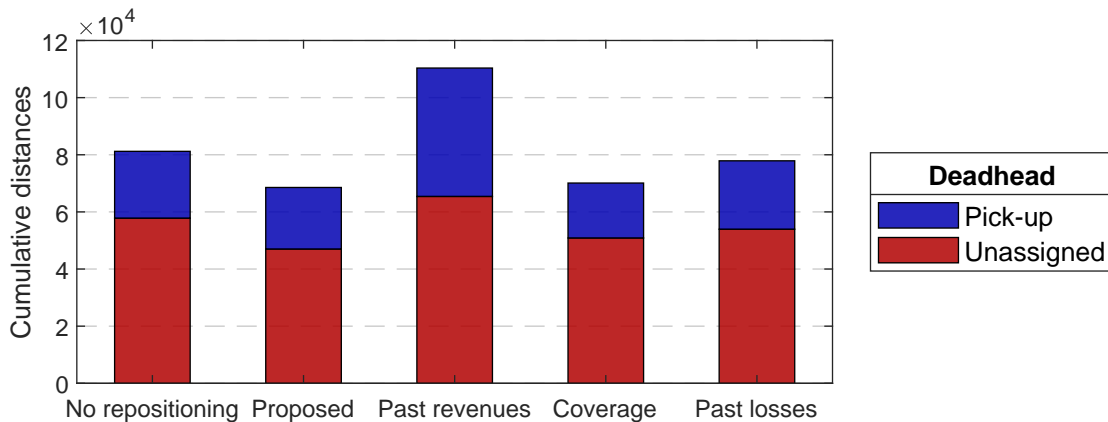


Figure 7: Summary of the deadhead associated with each repositioning strategy, separated into unassigned and pick-up kilometrages. Scenario with 2000 drivers and 50% of guidance rate in the ‘Proposed’ and ‘Past revenues’ methods.



## 5 CONCLUSIONS

In this paper we proposed a relocation strategy for ride-sourcing drivers by providing them with an estimate of their earnings. Therefore, we do not assume drivers unrestricted compliance to the provided guidance and, thus, they are free to make the decision that they expect will maximize their earnings. The first step in the proposed approach identifies the locations that are expected to maximize the chances of a driver getting a match in the forecast horizon. Then, a MDCTMC model is developed to capture the activities a driver will perform depending on his/her decision, which is later translated into an estimate of the driver's earnings. We showed that the proposed approach is likely to retain drivers confidence by improving their earnings compared to other drivers if the operator selects only a fraction of active drivers to provide guidance. Besides improving earnings, we show that the proposed approach manages to decrease the number of unserved requests in the system compared to several state-of-art benchmarks. It increased vehicle occupancy, and decreased the deadheading.

The findings provide a path for testing the impacts of different regulatory schemes in such systems. The provided guidance could further benefit drivers and unserved passengers, if it comes paired with other mechanisms to foster movements to poorly covered areas. It could include lower commissions in these areas, or other price changes to make it more attractive to drivers. Other research directions include developing optimal control to reposition without the decision-making process by drivers, which would be more realistic in cases with autonomous vehicles but it would also serve as upper (lower) bound for performance measurements and evaluation.

## REFERENCES

- Alonso-Mora, J., Samaranayake, S., Wallar, A., Frazzoli, E., & Rus, D. (2017). On-demand high-capacity ride-sharing via dynamic trip-vehicle assignment. *Proceedings of the National Academy of Sciences USA*, 114(3), 462–467. doi: 10.1073/pnas.1611675114
- Beojone, C. V., & Geroliminis, N. (2021). On the inefficiency of ride-sourcing services towards urban congestion. *Transportation Research Part C: Emerging Technologies*, 124, 102890. doi: 10.1016/j.trc.2020.102890
- Beojone, C. V., & Geroliminis, N. (2022). A dynamic multi-region mfd model for ride-sourcing systems with ridesplitting. *arXiv*, 2211.14560. doi: 10.48550/arXiv.2211.14560
- Ingolfsson, A. (2005). Modeling the M(t)/M/s(t) queue with an exhaustive discipline. *Working paper*. Retrieved from [http://www.bus.ualberta.ca/aingolfsson/working\\_papers.htm](http://www.bus.ualberta.ca/aingolfsson/working_papers.htm)
- Powell, J. W., Huang, Y., Bastani, F., & Ji, M. (2011). Towards reducing taxicab cruising time using spatio-temporal profitability maps. In D. Pfoser et al. (Eds.), *Advances in spatial and temporal databases* (pp. 242–260). Berlin, Heidelberg: Springer Berlin Heidelberg.
- Sadeghi, A., & Smith, S. L. (2019). On re-balancing self-interested agents in ride-sourcing transportation networks. In *2019 IEEE 58th Conference on Decision and Control (CDC)* (pp. 5119–5125). doi: 10.1109/CDC40024.2019.9030043
- Wang, H., & Yang, H. (2019). Ridesourcing systems: A framework and review. *Transportation Research Part B: Methodological*, 129, 122–155. doi: 10.1016/j.trb.2019.07.009
- Zhu, P., Sirmatel, I. I., Trecate, G., & Geroliminis, N. (2022). Distributed coverage control for vehicle rebalancing in mobility-on-demand systems. *TRB Annual Meeting*, 22-03340.